

# Multi-band accelerated high resolution population receptive field mapping on 7T

Allan Hummer<sup>A</sup>, Markus Ritter<sup>B</sup>, Michael Woletz<sup>A</sup>, Anna A. Ledolter<sup>B</sup>, Martin Tik<sup>A</sup>, Graham E. Holder<sup>C</sup>, Ursula Schmidt-Erfurth<sup>B</sup>, Christian Windischberger<sup>A</sup>

A. MR Physics Division, Center for Medical Physics and Biomedical Engineering, Medical University of Vienna, Vienna, Austria

B. Department of Ophthalmology and Optometry, Medical University of Vienna, Vienna, Austria

C. Department of Ophthalmology, National University of Singapore & National University Hospital, Singapore, Singapore

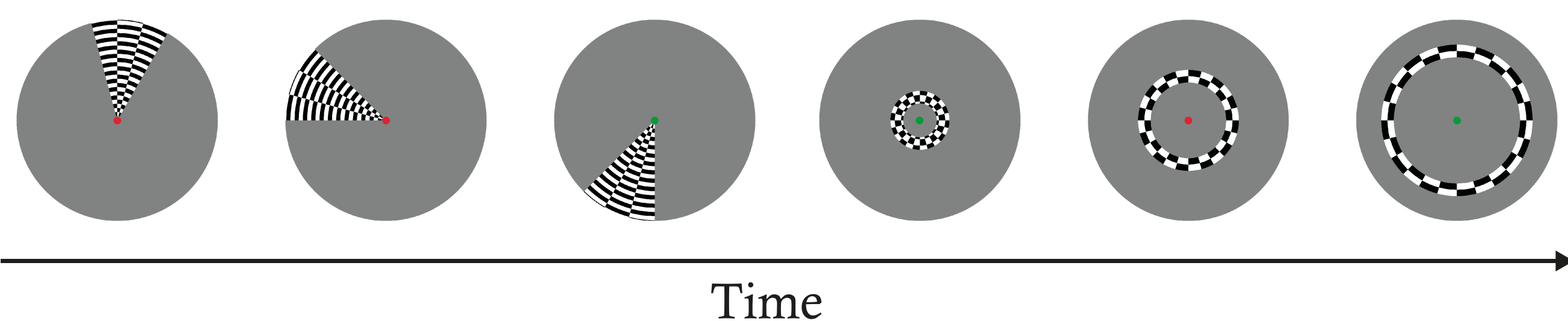
## Introduction

High resolution retinotopic imaging allows for accurate mapping of functional properties of the visual cortex. Among them, population receptive field (pRF) properties are of particular interest as recently demonstrated by in an investigation across cortical depth (Fracasso, A. 2016). Herein we employ a multi-band accelerated EPI sequence to increase sampling frequency and acquire retinotopic data with 0.8mm isotropic resolution at a repetition time of just 1 second. Despite sub-millimeter resolution this allowed us to acquire 336 volumes during a single 5 ½ minute scan.

## Methods

A 32-channel head coil was used to examine a group of 8 subjects (5 female; age  $24.8 \pm 3$ ) on a Siemens MAGNETOM 7T scanner. BOLD fMRI data of the visual cortex were acquired using the T2\*-weighted multi-band accelerated CMRR sequence (Moeller, S. 2010) with TE=23, TR=1000ms, voxel size=0.8mm isotropic, distance factor=10%, 36 slices, multiband factor=2, GRAPPA factor=3 and 336 volumes. Two runs were performed and slices were aligned orthogonally to the calcarine sulcus. A T1-weighted MPRAGE data set with 0.7mm isotropic resolution was also recorded. Subjects were presented with a combined wedge and ring retinotopic stimulus, covering the central 14° of the visual field, and instructed to fixate a small dot at the center of the screen during stimulus presentation. The visual cortex grey matter (GM) mask was generated based on MPRAGE data using automatic Freesurfer segmentation and manually corrected for topological errors with ITKGray. Preprocessing of fMRI data, i.e. slice-time correction, realignment and distortion correction using fieldmaps was performed with FSL, MATLAB and SPM12. mrVista was used for retinotopic model fitting by estimating a 2D Gaussian pRF model for each GM voxel. The primary visual cortex was delineated using phase reversals shown by polar angle maps on a three-dimensional mesh of the WM/GM border.

### Stimulus



### PRF Stability (Run 1 vs. Run 2)

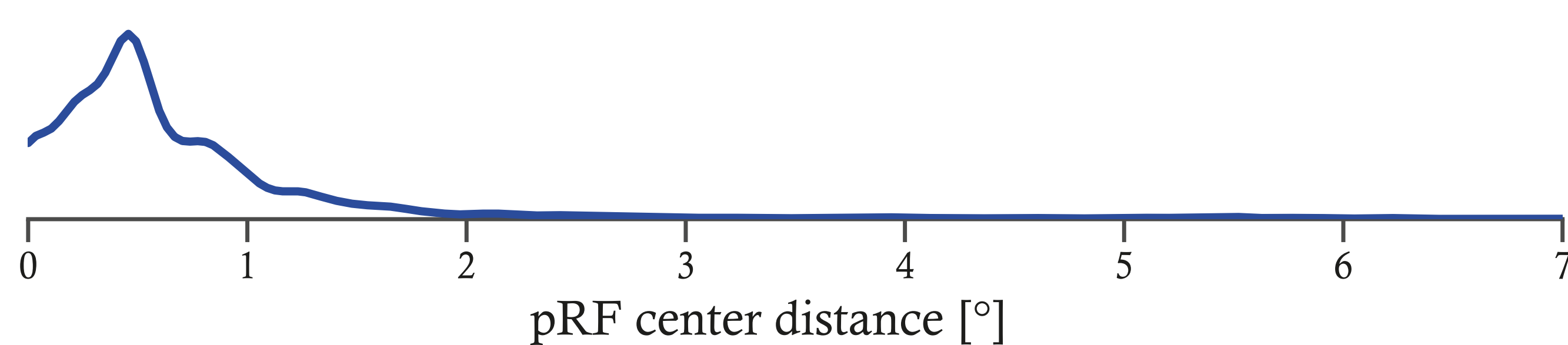


**Figure 1.** On top, the visual stimulus presented to the subjects is shown. A rotating wedge was alternated with an expanding ring, both revealing a flickering checkerboard. This sequence was repeated four times and interleaved with mean luminance pauses. Below, the probability density function of a voxelwise comparison between runs and with regard to the estimated pRF centers is shown.

## Wedges/Rings pRF Maps

V1 Left

Unsmoothed

Smoothed

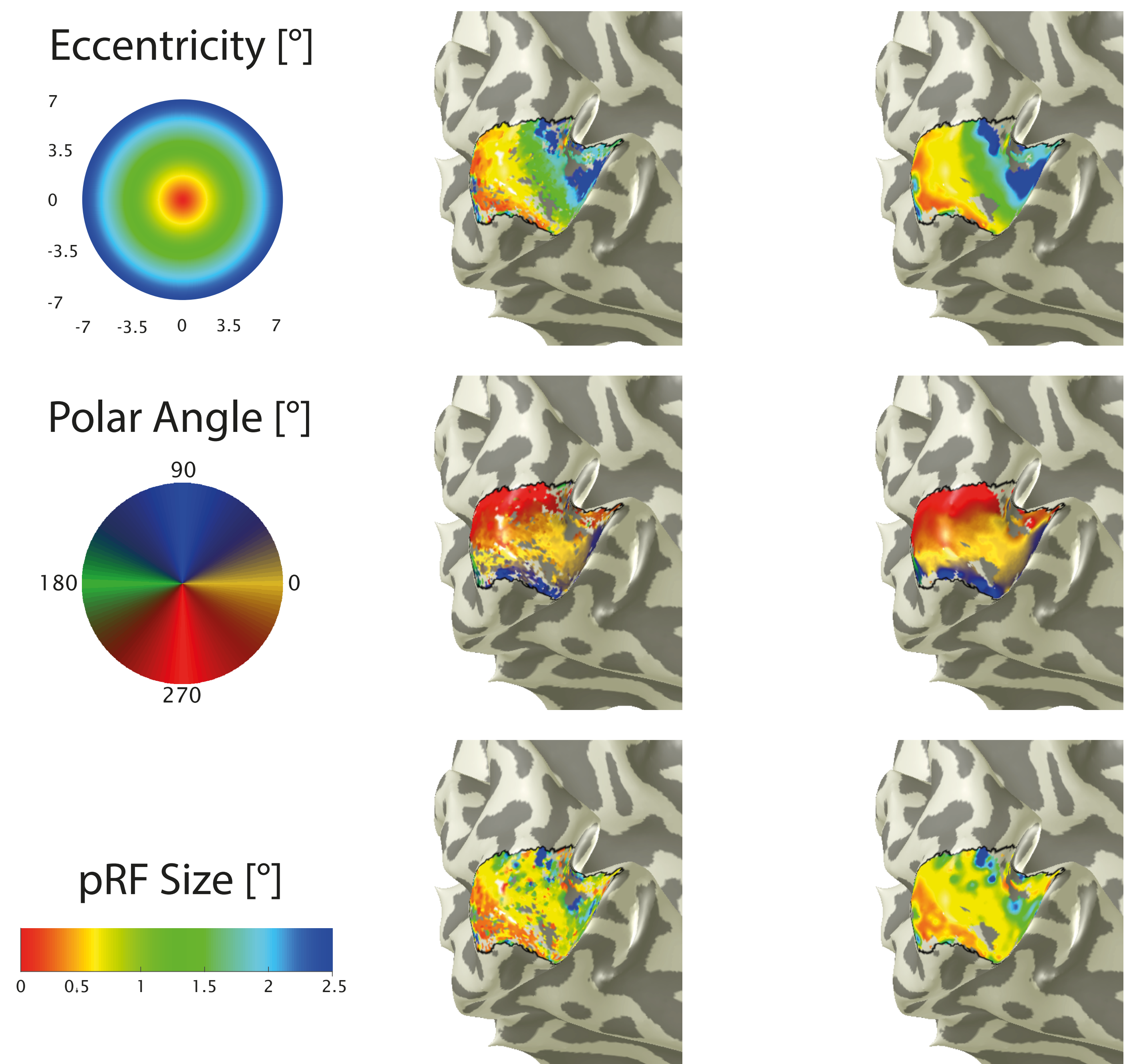


**Figure 2.** Estimated retinotopic maps of a subject overlaid on the left primary visual cortex. Data shown in the right column is smoothed using neighborhood averaging. All maps are thresholded at 1% explained variance.

## Results

Figure 1 depicts the visual stimulus time course on top. At the bottom, pRF stability is visualized by the distance of each voxel's estimated pRF center between runs (mean  $\pm$  std:  $0.77 \pm 1.06$ ). Figure 2 shows estimated pRF data of a single 5 ½ minute run, i.e. the estimated eccentricity, polar angle and pRF size, of one subject.

## Conclusion

Here, pRF mapping has been performed at ultra-high field with sub-millimeter spatial resolution and a TR of 1s. In clinical application, high spatial resolution could help to detect small details, e.g. small central scotoma in retinotopic maps, which would otherwise be obscured due to partial volume effects. Multiband acceleration can also be used to either increase acquisition speed, which decreases the risk of severe subject movement, or to acquire more data points in a given time, leading to an improved pRF model fit.

## References

- Fracasso, A. (2016). Systematic variation of population receptive field properties across cortical depth in human visual cortex, *NeuroImage*, vol. 139, pp. 427-438
- Moeller, S. (2010). Multiband multislice GE-EPI at 7 tesla, with 16-fold acceleration using partial parallel imaging with application to high spatial and temporal whole-brain fMRI, *Magnetic Resonance in Medicine*, vol. 63(5), pp. 1144-1153
- Hummer, A. (2018). Artificial scotoma estimation based on population receptive field mapping, *NeuroImage*, vol. 169, pp. 342-351
- Hummer, A. (2016). Eyetracker-based gaze correction for robust mapping of population receptive fields, *NeuroImage*, vol. 142, pp. 211-224

